



An Indirect PI-MPC Hybrid Method-Based Bi-quasi-Modified Switched Z Source Inverters for Vehicle to Grid applications

Anish Tiwari , Anandita Chowdhury 

Electrical Engineering Department (EED), Sardar Vallabhbhai National Institute of Technology, Surat, Gujarat, India

Cite this article as: A. Tiwari and A. Chowdhury, "An indirect PI-MPC hybrid method-based bi-quasi-modified switched Z source inverters for vehicle to grid applications," *Electrica*, 23(1), 20-27, 2023.

ABSTRACT

A comparative analysis on the performance of bi-quasi-modified switched Z source (Bi-qMSZSI) topology having a bidirectional attribute with the different control algorithm for the vehicle to grid interfacing utilizing proportional integral (PI) controller and Finite-set model predictive control (MPC) control was discussed in the study. The proposed work utilizes cascaded PI controllers and advanced MPC algorithm on a relatively new Bi-qMSZSI impedance source network topology. A total of four PI controllers or more may require to control the power exchange using the cascaded PI control technique. The tuning requirement for the cascaded PI controllers increases the overall control complexity, whereas the finite-set MPC algorithm generates switching pulses on the AC side in conjunction with a single PI controller on the DC side, reducing the burden. Adoption of finite-set MPC algorithm for discretized instantaneous model minimizes the current ripples prominent in cascaded PI control. Switched Z source inverter has a high boost factor with lesser passive elements compared to other impedance source network topologies. Bi-qMSZSI has an added advantage of constant DC link voltage with a finite set MPC Algorithm; it produces better results than cascaded PI controllers.

Index Terms—Indirect model predictive control (IMPC), finite set MPC, proportional integral (PI) controller, bi-quasi-modified switched Z source Inverter (Bi-qMSZSI), VSI, shoot-through state, modulation index (m) and duty (D) cycle

Corresponding author:

Anish Tiwari

E-mail:

anishtiwari283@gmail.com

Received: December 15, 2021

Revised: April 18, 2022

Accepted: May 9, 2022

Publication Date: September 26, 2022

DOI: 10.5152/electrica.2022.21177



Content of this journal is licensed under a Creative Commons Attribution-NonCommercial 4.0 International License.

I. INTRODUCTION

With the advent of electric vehicles, there comes a need for reliable charging infrastructure. While designing the charging infrastructure for the distribution network, reactive power compensation functionality becomes crucial. A typical station operation would fast charge the vehicle and provide ancillary services when demanded by the network operator [1-4].

The present control strategy is proposed to utilize the reactive power compensation capability of the electric vehicle charger for the balanced and unbalanced distribution network. Reactive power compensation is performed for the distribution networks to keep node voltages within safe operating limits. Increasing renewable penetration makes distribution networks more vulnerable to voltage variations. Hence, there is a need for compensating the reactive power. Advanced compensation equipment is quite expensive for a small distribution network; therefore, utilizing the power electronics circuitry of the electric vehicle is an acceptable alternative [5-9].

Usually, the vehicle-to-grid or grid-to-vehicle concept requires a bidirectional converter topology for power exchange. In traditional Voltage Source Inverter (VSI), dead-time avoids short circuit failure but distorts the ac output voltage waveform [10]. Z source inverter topology has a unique X-shaped network in between DC source terminals [11] that eliminates this need for dead-time for short-circuit fault protection, making itself a potential choice for bidirectional power exchange [12]. Switched Z source inverters [13] provide a better boost compared to conventional Z source. It also possesses all the advantages of the traditional one with a reduced duty ratio (D) range enabling more margin for modulation index (m). Further modifications to this topology result in constant DC link operation, making it a direct replacement of VSI in a variety of power conversion applications [14].

The finite set model predictive control algorithm is easy to implement and adopted widely for power converter applications. It is a form of a single-step optimization control where the

multivariable objective function defines different variables and identifies the minimum switching vector. Finite-set model predictive control (MPC) is a good choice for applications dealing with double frequency oscillations due to the unbalanced loading. It is possible to eliminate the double frequency component considering three variables in the objective function. The control gives superior performance over conventional PI control for single-step prediction horizon. The presence of two variables in the objective function reduces the computational burden significantly to about 50%. The method is only applicable to the converters where the inductor current is not related to the converter current. A single PI controller provides proportional action with an objective function utilizing the concept of maxima and minima to generate an appropriate voltage vector on the grid side [15-20].

The following points are considered a contribution to the study presented:

1. Bidirectional power exchange between Electric Vehicle (EV) batteries and the grid analyzed for balanced grid operation using PI controller in bidirectional quasi-modified Switched Z source inverter (Bi-qMSZSI).
2. The indirect predictive control algorithm reduces the overall computational complexity by eliminating the need for PI controllers on the AC side.
3. Utilizing a single PI controller instead of a cascaded PI control further reduces the computational requirement.

The upcoming sections organized under Section I are about the system description. Section II deals with power calculations in the stationary reference frame and Section III mentions various reference current generation methods for unbalanced operating conditions. The conventional PI control method and predictive control theory details with optimization technique flowchart and overall methodology are shown in Section IV, whereas Section V discusses simulation and results. Section VI is the conclusion derived from the simulation results and references cited last.

II. SYSTEM DESCRIPTION

The system Fig. 1 comprises batteries, two inductors $L_{1,2}$ in quasi-Z source arrangement, three capacitors $C_{1,2,0}$, and a total of five bidirectional IGBT switches to form a modified switched Z source network. The output DC link connects the H-bridge that indeed links filter inductors to three-phase grid for vehicle to grid power exchange.

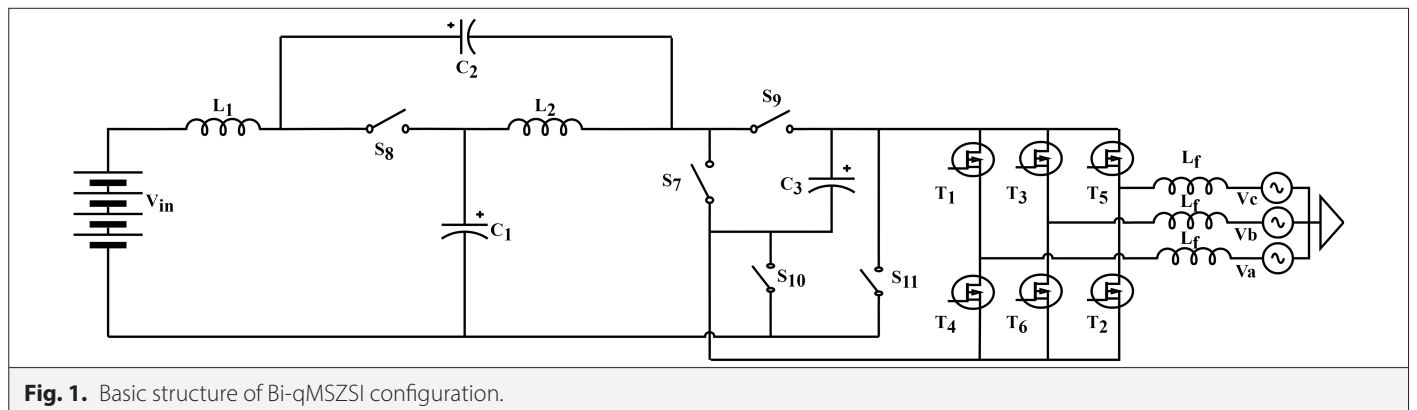


Fig. 1. Basic structure of Bi-qMSZSI configuration.

III. INSTANTANEOUS POWER CALCULATIONS

Three-phase instantaneous power is expressed as given in the following equation, and voltages are measured from a fictitious star point since the three-phase three wire system is without a neutral point.

$$P_{3\phi} = v_a(t) * i_a(t) + v_b(t) * i_b(t) + v_c(t) * i_c(t) \quad (1)$$

A. Power Theory for Balanced Grid Condition

Considering the completely balanced conditions, the instantaneous complex power S is defined as the product of voltage vector $\rightarrow \bar{v}$ conjugate of the current vector i^* .

$$S = \bar{v} * i^* = (v_\alpha + j * v_\beta) * (i_\alpha - j * i_\beta) \quad (2)$$

The real and imaginary terms of complex power in (2) can be rewritten as follows when the power invariant is taken into account:

$$\begin{Bmatrix} p \\ q \end{Bmatrix} = \frac{3}{2} \begin{Bmatrix} v_\alpha & v_\beta \\ -v_\beta & v_\alpha \end{Bmatrix} * \begin{Bmatrix} i_\alpha \\ i_\beta \end{Bmatrix} \quad (3)$$

In matrix form, the instantaneous reference currents can be expressed as given below:

$$\begin{Bmatrix} i_\alpha^* \\ i_\beta^* \end{Bmatrix} = \frac{2}{3} * \frac{1}{(v_\alpha^2 + v_\beta^2)} * \begin{Bmatrix} v_\alpha & v_\beta \\ v_\beta & -v_\alpha \end{Bmatrix} * \begin{Bmatrix} p \\ q \end{Bmatrix} \quad (4)$$

IV. CONTROL METHODOLOGY

A. Conventional Control Method

The conventional control strategy, in Fig. 2, utilizes cascade PI control having outer voltage and inner current loops on the DC side. To extract θ angle for the transformation of grid voltages and currents, the Synchronous reference frame phase-locked loop (SRF-PLL) senses the three-phase grid voltages. The reference current generation for the PI controllers on the AC side utilizes Eq. 4. The processed error generates reference voltages that further produce the modulating signals to get PWM switching pulses.

B. Direct and Indirect Predictive Control Algorithm

The direct model predictive control (DMPC) utilizes optimal switching vectors. After many iterations, the cost function gets optimized, resulting in desired switching vector selection. On the other hand, indirect model predictive control (IMPC) does not need iterative

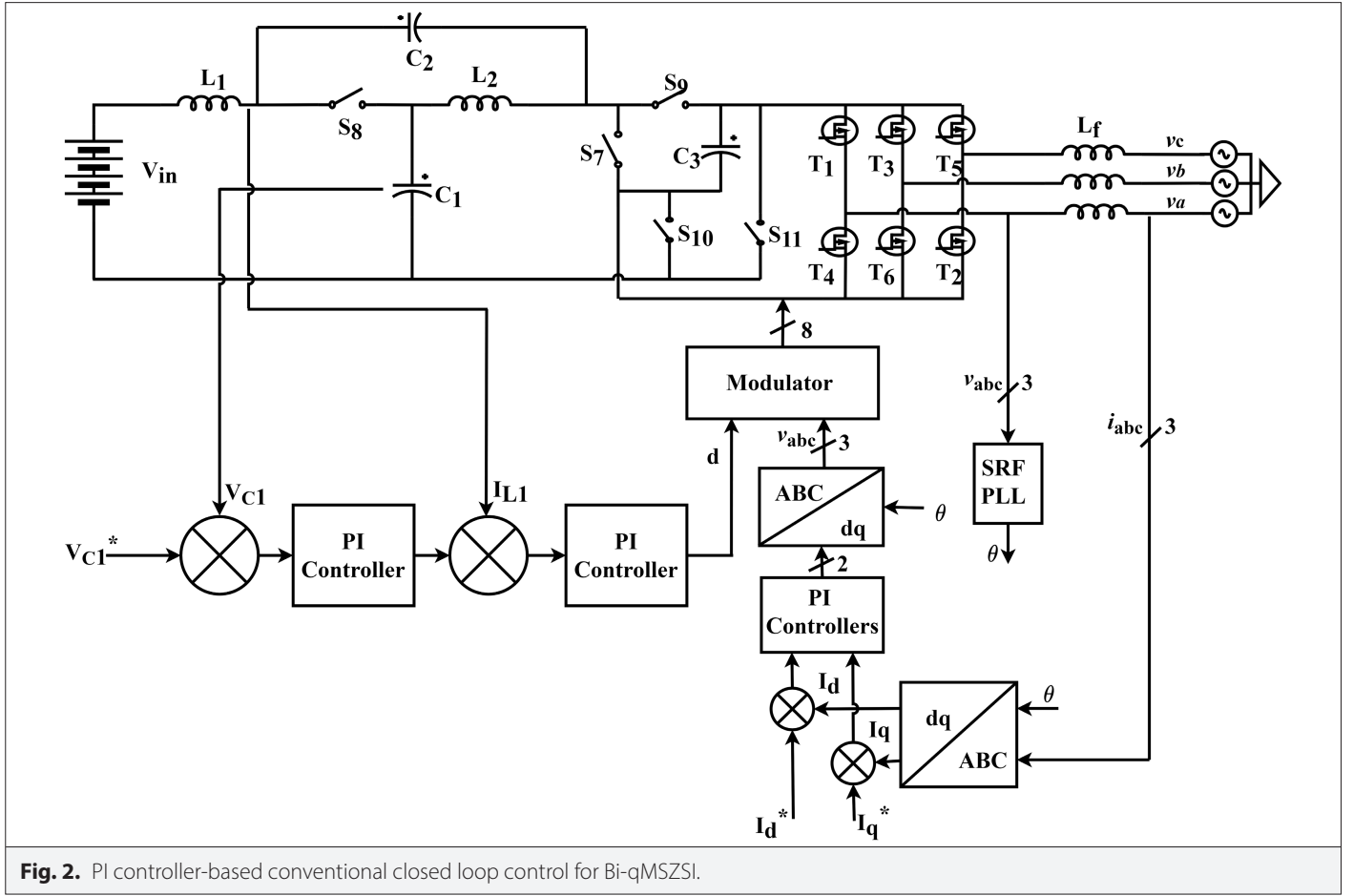


Fig. 2. PI controller-based conventional closed loop control for Bi-qMSZSI.

switching vector selection. In DMPC, complete discretization should be on both the DC and AC sides, whereas, in IMPC, only AC discrete model equations are involved, and single PI control is sufficient on the DC side. Since modified switched Z source topology (MSZSI) is similar to conventional VSI operation, a discrete model of the whole system is not required. Hence, the IMPC method is well suited for its operation.

The MPC algorithm, Fig. 3, structure gives a brief flow for code generation. The grid currents give the initial value for formulating the quadratic objective function. Optimization techniques select the minimum value after the number of iterations. The single-step algorithm always gives the minimum value after optimization.

In a stationary reference $\alpha - \beta$ frame, the predictive three-phase grid current is expressed as:

$$\begin{aligned} i_{\alpha(m+1)} &= \left(1 - \frac{R_f * T_s}{L_f}\right) * i_{\alpha(m)} + \frac{T_s}{L_f} * [V_{inv,\alpha(m)} - v_{\alpha(m)}] \\ i_{\beta(m+1)} &= \left(1 - \frac{R_f * T_s}{L_f}\right) * i_{\beta(m)} + \frac{T_s}{L_f} * [V_{inv,\beta(m)} - v_{\beta(m)}] \end{aligned} \quad (5)$$

The quadratic cost function can be written as follows:

$$C = C_\alpha + C_\beta = |i_{\alpha(m+1)}^* - i_{\alpha(m)}|^2 + |i_{\beta(m+1)}^* - i_{\beta(m)}|^2 \quad (6)$$

The above expression upon partial differentiation gives the minimum value

$$\begin{aligned} \frac{\partial C}{\partial V_{inv,\alpha}} &= 0 \\ \frac{\partial C}{\partial V_{inv,\beta}} &= 0 \end{aligned} \quad (7)$$

The minimum grid voltage vector in the stationary frame of reference derived from the above equation can be expressed as:

$$V_{\alpha,min} = -\frac{L_f}{T_s} * \left[\left(1 - \frac{R_f * T_s}{L_f}\right) * i_{\alpha(m)} + \frac{T_s}{L_f} * v_{\alpha(m)} - i_{\alpha(m+1)}^* \right] \quad (8)$$

$$V_{\beta,min} = -\frac{L_f}{T_s} * \left[\left(1 - \frac{R_f * T_s}{L_f}\right) * i_{\beta(m)} + \frac{T_s}{L_f} * v_{\beta(m)} - i_{\beta(m+1)}^* \right] \quad (9)$$

The overall MPC control topology comprises only one PI control on the DC side as shown in Fig. 4. Instead of the conventional reference current equation, the above control utilizes (8) and (9). The transformed voltages and current obtained through Clark transformation were fed directly to the finite-set MPC control algorithm. The optimized values in the stationary reference frame are utilized to produce a modulation index, which generates the switching pulses.

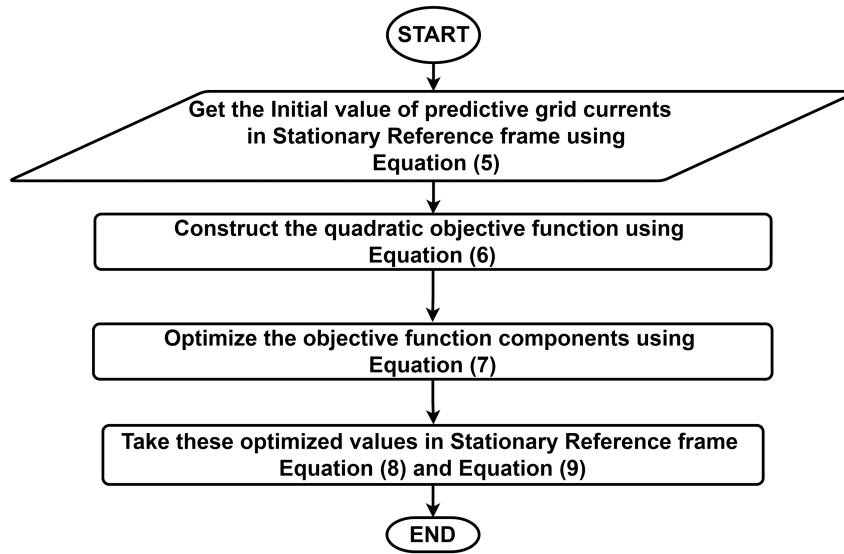


Fig. 3. Flowchart of indirect MPC-based algorithm for Bi-qMSZSI.

V. SIMULATION AND RESULTS

Upon analysis of the Bi-qMSZSI topology with the battery input voltage variations and the converter’s response with a 20% dip seen in Fig. 5(a) and a 20% surge seen in Fig. 5(b), the duty ratio is also varying in accordance to compensate it. The closed loop PI control for the

converter is designed to give 2.5 times boost at duty value $D = 0.15$. The converter can sustain the variations without considerably affecting the inductor switching ripples.

Finite-set MPC control for the Bi-qMSZSI topology produces similar results for battery voltage variations as Fig. 6(a) shows 20% dip

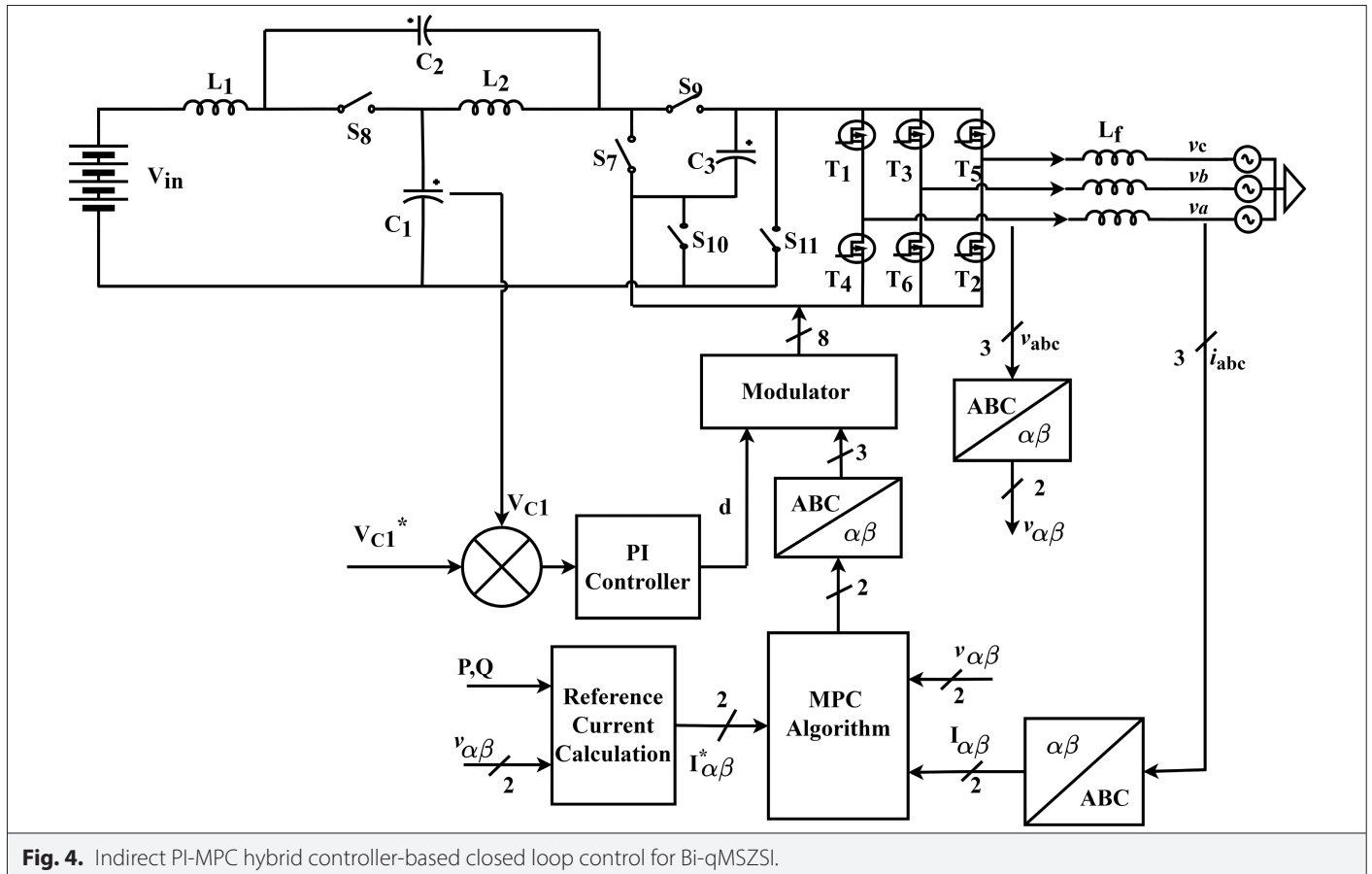


Fig. 4. Indirect PI-MPC hybrid controller-based closed loop control for Bi-qMSZSI.

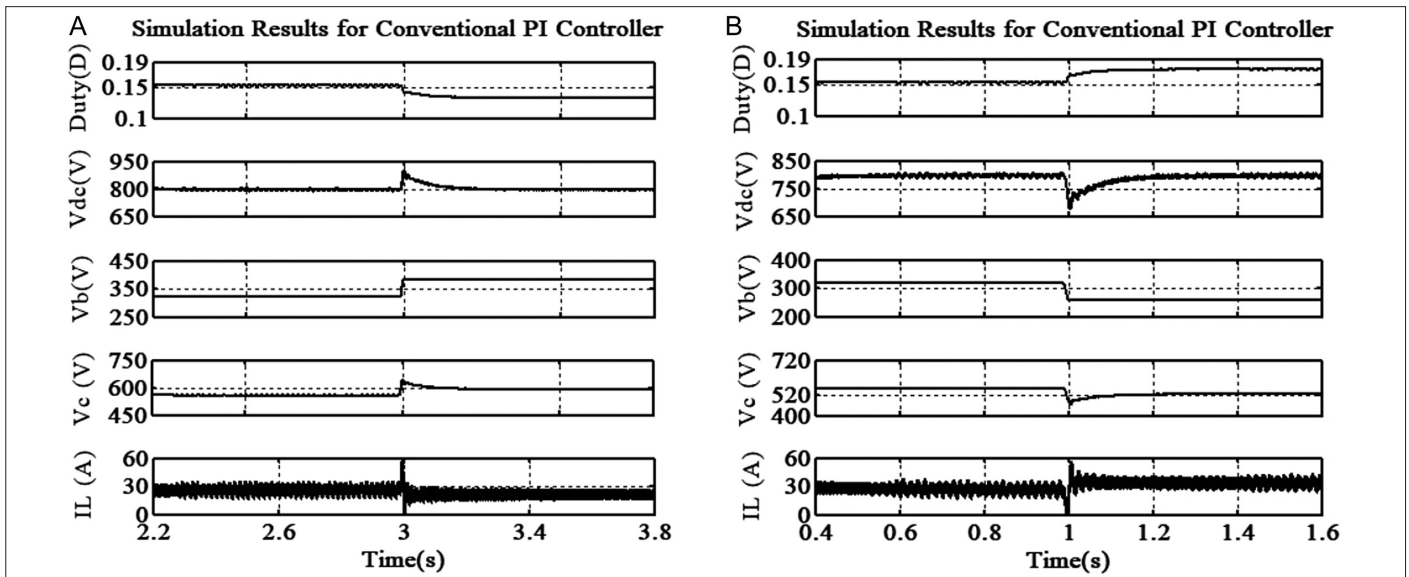


Fig. 5. (a) Input battery voltage variations for conventional PI controllers with 20% fall in battery voltage. (b) Input battery voltage variations for conventional PI controllers with 20% rise in battery voltage.

and Fig. 6(b) 20% rise. The duty ratio in the first and second cases increases and decreases to compensate for the variations. Upon observation, the switching ripples with MPC control were minimal when compared with PI controller.

The results with the PI controller on the grid side validate the bidirectional attribute of the Bi-qMSZSI topology. Figure 7(a) shows an active power exchange of 6 kW before and after the step change during which the battery delivers power to the grid represented by in-phase operation and vice versa represented by out-of-phase operation. Figure 7(b) shows the reactive power exchange of 6 kVAR before and after step change. The converter

provides leading reactive power capacitive operation and lagging reactive power inductive operation. Better performance is observed with an MPC controller on the grid control side. Figure 8(a) shows active power of 1 kW transition before and after the step change representing power exchange from the battery toward the grid and vice versa. In Fig. 8(b), before and after the step change, inductive lagging reactive power and capacitive leading the reactive power of 1 kVAR were provided by the converter to the grid.

Table I shows technical analysis in terms of the different parameters such as boost factor, proportional and integral gain tuning, the need

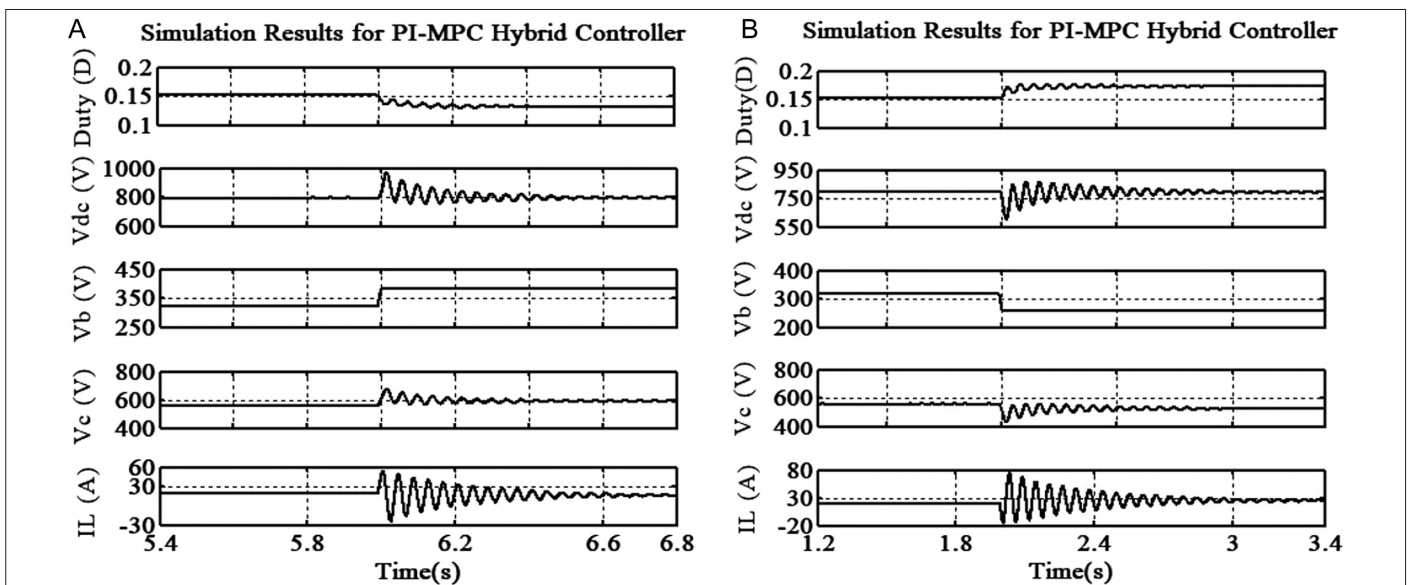


Fig. 6. (a) Input battery voltage variations for PI-MPC hybrid controllers with 20% fall in battery voltage. (b) Input battery voltage variations for PI-MPC hybrid controllers with 20% rise in battery voltage.

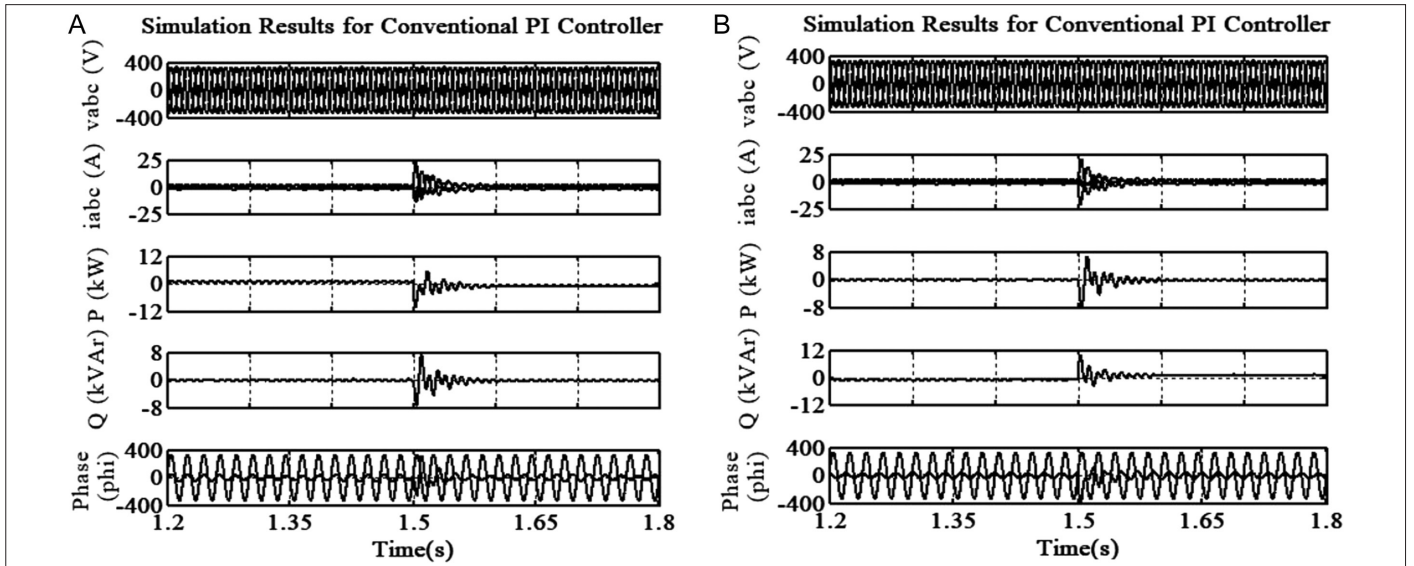


Fig. 7. (a) Power variations for conventional PI controllers with active power transfer from grid to battery and vice versa. (b) Power variations for conventional PI controllers with reactive power transfer from grid to battery and vice versa.

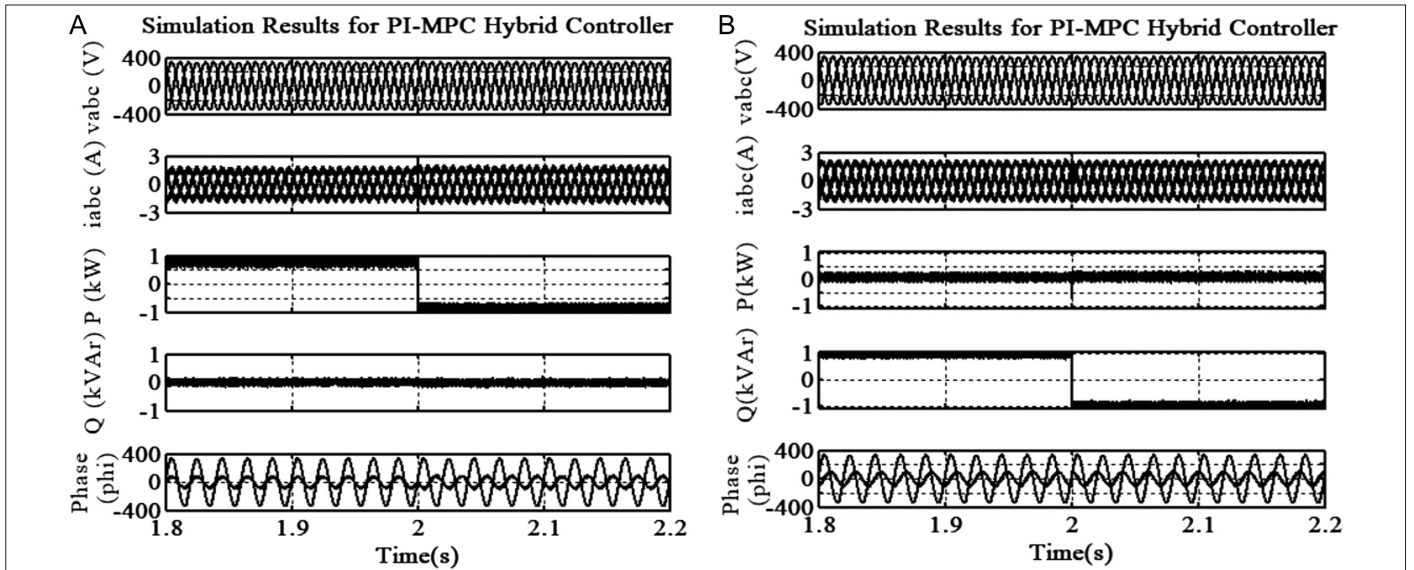


Fig. 8. (a) Power variations for indirect PI-MPC hybrid controllers with active power transfer from grid to battery and vice versa. (b) Power variations for indirect PI-MPC hybrid controllers with reactive power transfer from grid to battery and vice versa.

TABLE I. SUMMARY OF SIMULATION RESULTS FOR VARIOUS CONTROL TECHNIQUES

S. No.	Type of Converter	Parameters	Conventional Control Method	Indirect Model Predictive Control PI-MPC Hybrid Algorithm
1	Bidirectional quasi-modified switched Z source inverter	Constant DC link	Yes	Yes
		High boost factor	Yes	Yes
		Bidirectional attribute	Yes	Yes
		Transients during power exchange	Very high	Very low
		PI tuning requirement	Very high	Very low
		PLL required for grid synchronization	Yes	No

PI-MPC, proportional integral model predictive control.

for a phase lock loop for grid angle extraction, and the smooth power exchange between vehicle to grid and grid to vehicle.

VI. CONCLUSION

The present work suggests that the Bi-q-MSZSI topology with the conventional PI controller's closed-loop control has a higher amplitude of transient peaks during the power transition and produces more switching ripples in the battery current. Prolonged use of the battery in such conditions may deteriorate its life cycle. On the other hand, the finite-set MPC algorithm reduces switching ripples in battery current and eliminates transient peaks during a power transition, as evident from the results. The smooth active/reactive power transition between the battery and the grid suggests that the Bi-qMSZSI topology performs better with the proposed indirect PI-MPC hybrid control algorithm than with the conventional PI controller

Peer-review: Externally peer-reviewed.

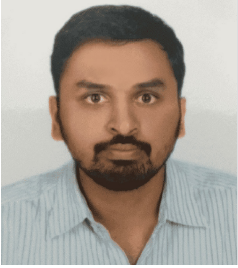
Author Contributions: Concept – A.T., A.C.; Design – A.T., A.C.; Data Collection and/or Processing – A.T., A.C.; Analysis and/or Interpretation – A.T., A.C.; Literature Review – A.T., A.C.; Writing – A.T., A.C.

Declaration of Interests: The authors declare that they have no competing interest.

Funding: The authors declared that this study has received no financial support.

REFERENCES

1. Y. Ota, H. Taniguchi, T. Nakajima, K. M. Liyanage, J. Baba, and A. Yokoyama, "Autonomous distributed V2G (vehicle-to-grid) satisfying scheduled charging," *IEEE Trans. Smart Grid*, vol. 3, no. 1, pp. 559–564, 2011. [\[CrossRef\]](#)
2. W. Kempton, and A. Dhanju, "Electric vehicles with V2G," *Windtech Int.*, vol. 2, no. 2, p. 18, 2006.
3. U. K. Madawala, and D. J. Thrimawithana, "A bidirectional inductive power interface for electric vehicles in V2G systems," *IEEE Trans. Ind. Electron.*, vol. 58, no. 10, pp. 4789–4796, 2011. [\[CrossRef\]](#)
4. C. Zhou, K. Qian, M. Allan, and W. Zhou, "Modeling of the cost of EV battery wear due to V2G application in power systems," *IEEE Trans. Energy Convers.*, vol. 26, no. 4, pp. 1041–1050, 2011. [\[CrossRef\]](#)
5. B. Bibak, and H. Tekiner-Moğulkoç, "A comprehensive analysis of Vehicle to Grid (V2G) systems and scholarly literature on the application of such systems," *Renew. Energy Focus*, vol. 36, pp. 1–20, 2021. [\[CrossRef\]](#)
6. C. Guille, and G. Gross, "A conceptual framework for the vehicle-to-grid (V2G) implementation," *Energy Policy*, vol. 37, no. 11, pp. 4379–4390, 2009. [\[CrossRef\]](#)
7. J. Hu, C. Ye, Y. Ding, J. Tang, and S. Liu, "A distributed MPC to exploit reactive power V2G for real-time voltage regulation in distribution networks," *IEEE Trans. Smart Grid*, vol. 13, no. 1, pp. 576–588, 2021.
8. H. Lund, and W. Kempton, "Integration of renewable energy into the transport and electricity sectors through V2G," *Energy Policy*, vol. 36, no. 9, pp. 3578–3587, 2008. [\[CrossRef\]](#)
9. B. K. Sovacool, and R. F. Hirsh, "Beyond batteries: An examination of the benefits and barriers to plug-in hybrid electric vehicles (PHEVs) and a vehicle-to-grid (V2G) transition," *Energy Policy*, vol. 37, no. 3, pp. 1095–1103, 2009. [\[CrossRef\]](#)
10. H. Abu-Rub, M. Malinowski, and K. Al-Haddad, *Power Electronics for Renewable Energy Systems, Transportation and Industrial Applications*. Chichester: John Wiley & Sons, 2014.
11. F. Z. Peng, "Z-source inverter," *IEEE Trans. Ind. Appl.*, vol. 39, no. 2, pp. 504–510, 2003. [\[CrossRef\]](#)
12. W. Xu, K. W. Chan, S. W. Or, S. L. Ho, and M. Liu, "A low-harmonic control method of bidirectional three-phase Z-source converters for vehicle-to-grid applications," *IEEE Trans. Transp. Electrification*, vol. 6, no. 2, pp. 464–477, 2020. [\[CrossRef\]](#)
13. J. Liu, J. Wu, J. Qiu, and J. Zeng, "Switched Z-source/quasi-Z-source DC-DC converters with reduced passive components for photovoltaic systems," *IEEE Access*, vol. 7, pp. 40893–40903, 2019. [\[CrossRef\]](#)
14. A. Tiwari, and A. Chowdhury, "Modified switched Z-source topology for inverter applications," in *Lecture Notes in Electrical Engineering, Proceedings of Symposium on Power Electronic and Renewable Energy Systems Control*, pp. 31–41, 2021. [\[CrossRef\]](#)
15. N. Jin, C. Gan, and L. Guo, "Predictive control of bidirectional voltage source converter with reduced current harmonics and flexible power regulation under unbalanced grid," *IEEE Trans. Energy Convers.*, vol. 33, no. 3, pp. 1118–1131, 2017. [\[CrossRef\]](#)
16. A. Bakeer, M. A. Ismeil, and M. Orabi, "A powerful finite control set-model predictive control algorithm for quasi Z-source inverter," *IEEE Trans. Ind. Inform.*, vol. 12, no. 4, pp. 1371–1379, 2016. [\[CrossRef\]](#)
17. S. Bayhan, M. Trabelsi, H. Abu-Rub, and M. Malinowski, "Finite-control-set model-predictive control for a quasi-Z-source four-leg inverter under unbalanced load condition," *IEEE Trans. Ind. Electron.*, vol. 64, no. 4, pp. 2560–2569, 2016. [\[CrossRef\]](#)
18. O. Ellabban, J. van Mierlo, and P. Lataire, "A DSP-based dual-loop peak DC-link voltage control strategy of the Z-source inverter," *IEEE Trans. Power Electron.*, vol. 27, no. 9, pp. 4088–4097, 2012. [\[CrossRef\]](#)
19. H. S. Molina, J. D. Rojas, and L. M. Tamayo, "Finite set model predictive control to a shunt multilevel active filter," *COMPEL Int. J. Comput. Math. Electr. Electron. Eng.*, vol. 34, no. 1, pp. 279–300, 2015.
20. R. Alla, and A. Chowdhury, "Model predictive controller for improved hybrid three quasi Z source inverter for DG applications," in *IEEE International Conference on Power Electronics, Drives and Energy Systems (PEDES)*, 2018, pp. 1–6.



Anish Tiwari received the B.E. Electrical and Electronics degree from Rajiv Gandhi Proudyogiki vishwavidhyalaya, Bhopal, India, in 2012 and M.E. Power Systems from UIT-RGPV Bhopal India in 2015. Currently, he is pursuing a Doctoral degree in Electrical Engineering at Sardar Vallabhbai National institute of technology Surat, India, from December 2018. His current research area includes Electric vehicle, Power Converters, and their applications, Power electronics, and impedance source networks.



Anandita Chowdhury received her B.E. and M.E. degrees from the University of Calcutta and her Ph.D. degree from the Indian Institute of Technology, Kharagpur. Presently, she is working as a Professor in the Department of Electrical Engineering of S. V. National Institute of Technology, Surat, India. She has more than twenty-five years of teaching experience. Her areas of research interest include electrical machines, drives, and power system stability.